ISSN 1392-1207. MECHANIKA. Vol. 31, No. 4, 2025: 389–395

Less Channel Hitting Measuring System for Table Tennis Monitoring

Chengjian HUA*, Xujie HU*, Zile FAN*, Weining FEI**
**School of Marxism Studies, Yiwu Industrial and Commercial College, Yiwu, Zhejiang 322000, China*
***School of Public Instruction, Wenzhou Polytechnic, Whenzhou, Zhejiang 325035, China, E-mail: full121314@163.com*
https://doi.org/10.5755/j02.mech.40463

1. Introduction

The integration of Artificial Intelligence (AI) with wearable devices is revolutionizing various fields, particularly in the realm of health monitoring and sports [1]. Wearable devices offer valuable insights into the human body, continuously collecting data, while AI methods enhance the ability to analyze this data efficiently and accurately [2]. This combination has been widely applied in areas such as disease diagnosis [3], continuous health monitoring [4], emotion sensing [5], and sports monitoring [6, 7]. However, despite the growing adoption of AI and wearables in health, their use in sports monitoring remains underdeveloped.

One of the challenges faced in sports monitoring lies in the limitations of the number of detectable points, which impacts the precision of data collection [8]. Achieving accurate measurements typically requires information from more detection points, necessitating the placement of additional sensors at these positions [9]. However, current detection technologies are constrained by the need to associate each detection point with a transmission channel [10]. This requires scaling up hardware, complicating the system and integration efforts. Furthermore, as the demand for more detailed information increases, the need to incorporate a variety of sensors into wearable devices grows, which places further strain on the system's signal channels [11]. Thus, there is a growing need for strategies that can reduce the number of signal pathways while maintaining the quality of data collection[12].

On the other hand, during sports, particularly in activities like table tennis, understanding the fatigue state of muscles is crucial for both physical and cognitive performance [13, 14]. Muscle fatigue is often linked to a decline in movement velocity or skill level during extended periods of activity, increasing the likelihood of injury. Monitoring muscle state provides valuable insights into exercise intensity, enabling athletes and trainers to adjust training loads, repetitions, and rest periods accordingly [15]. Real-time feedback on muscle fatigue can also enhance performance and reduce injury rates [16]. Traditional methods of assessing muscle status, such as biochemical tests or neuromuscular function assessments (e.g., EMG), are typically cumbersome and not ideal for continuous, real-time monitoring [17]. To address these limitations, wearable devices that track player movement are increasingly being utilized for non-contact, real-time monitoring of muscle fatigue [18]. Moreover, in table tennis, monitoring only the ball velocity does not offer a complete picture of an athlete's fatigue level. Techniques in table tennis rely not only on the ball's velocity but also on its rotation [19]. Wearable devices are capable of detecting the pressure variations on the racket caused by both ball velocity and rotation, providing a more comprehensive understanding of player performance and muscle fatigue [20].

This paper aims to explore these two aspects within the context of table tennis. Firstly, we propose a novel approach to reducing the number of signal channels required for measurement by using a soft piezoelectric device. This device, which converts kinetic energy into electrical energy, is used to measure the hitting force and ball contact points [21, 22]. By decomposing the sensing matrix into rows and columns, we reduce the signal channels from the traditional $m \times n$ to $m+n$, allowing for more efficient data collection. Secondly, we investigate the potential of using electromyography (EMG) signals to analyze the relationship between hitting force and muscle fatigue. A k-Nearest Neighbors (kNN) algorithm is employed to build a model that distinguishes whether data was collected at the beginning or after two hours of play, providing deeper insights into muscle fatigue and performance monitoring in sports.

In the first section, the background and motivation of this work are introduced. Then, the design, structures, and investigation of the fabricated on-racket sensing are shown in section 2. In section 3, the collected data from the racket in the real table tennis game can be found. To collect enough data for building a kNN training, EMG tests are conducted to form the status marker of the player. In section 4, the results of EMG tests are shown. The conclusion of the paper can be found in the final part. Overall, this work provides a method to reduce the number of signal channels in the piezoelectric sensing array, as well as build a system to detect the status of table tennis players using the system on the racket.

2. Design and Fabrication of the On-Racket Sensing System

When a table tennis hit the racket, the racket provides a force to the ball as well as collects the energy during the hitting. The fatigue of player leads to a decline in sporting performance, where this decline is manifested through the pressure exerted on the racket during gameplay [14]. By analyzing the collected pressure data on the racket, we aim to obtain not only the hitting information but also to get the further information about the players. In Fig. 1, a, this sensing concept is illustrated, while the structure of existed hitting measuring system and proposed system are in Fig. 1, b. If a 3×3 sensor array is employed in measurement, with each position housing a position to be monitored [23], most of the existing designs relies on an individual signal channel for each sensor, which will connect the communication module and transmit the information out. Then, hardware for 9 information traces is needed [24]. For the proposed less signal channel designs, the hitting position is searched by its row

and column coordinates. Each row and column are connected together and only 6 output channels are needed by using the new design. The conceptual design can also be scall up, where the needed information transmission hardware for building $m \times n$ sensing units will drop from $m \times n$ to $m+n$.

Along with the designing method, the on-racket sensing system is fabricated using a standard table tennis racket as the framework. Six cross-arranged sensors are affixed to its surface to form a 3×3 sensing array, where each sensing position has two lines to connect the interface circuit: one for the row and one for the column. A picture of the fabricated system is shown in Fig. 2, a. Given the lightweight nature of the table tennis ball, the impact of the racket alone is insufficient to power the circuit. Therefore, two commercial 1.5 V AAA batteries are employed to supply the necessary power. Six PVDF striped sensors (from LOXGO company, shown in the insert depicts in Fig. 2, a) are used, where three of them are arranged as horizontal sensing elements at the bottom (sensor 1-3) and the others are vertical sensing elements on the top (sensor 4-6). The sensors with size of 1 cm wide and 8 cm long, are crossly sited, where the distance of 2.5 cm with each other to cover the enough racket surface. These sensors are affixed to the surface of the racket rubber film and shielded with a protective layer. The circuit details are illustrated in Fig. 2, b. All six sensors are connected in parallel to the sensing circuit chip, which comprises a CC1350 Bluetooth Micro Control Unit (MCU) with an RF-IC antenna. Voltage changes from all six sensing channels are transmitted to a personal computer (PC). The primary circuit operates on power from the battery. The sampling frequency is set at 128 kHz, with a transmitting frequency of 1 GHz.

After all the elements for the whole system are prepared, we did the final assembling carefully: the battery were embed into the wood handle of the racket by a proper

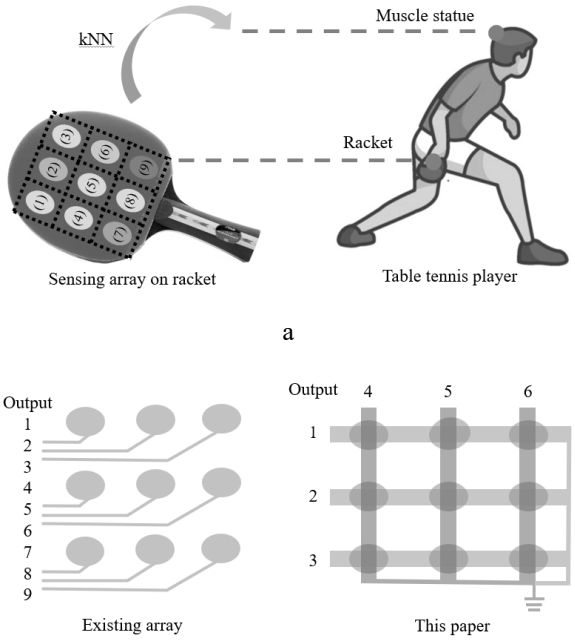

Fig. 1 Demonstration of the less channel on-racket table tennis monitoring: a – racket hitting force for players' fatigue quantification, b – comparation of the existing point-to-point measurement system and proposed less signal channel measurement system

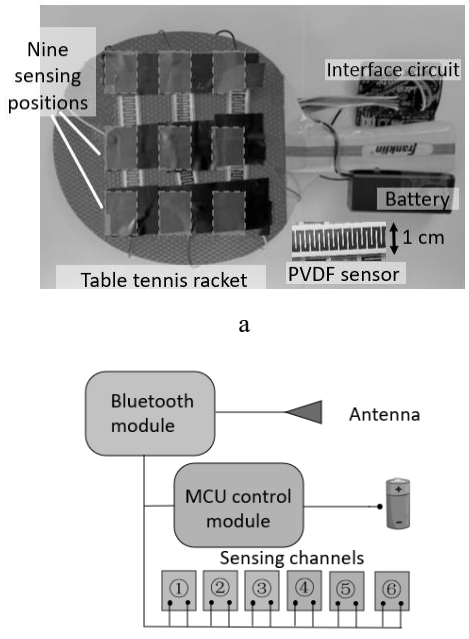

Fig. 2 Structure and design of the on-racket table tennis monitoring system: a – picture of the fabricated system, b – circuit design

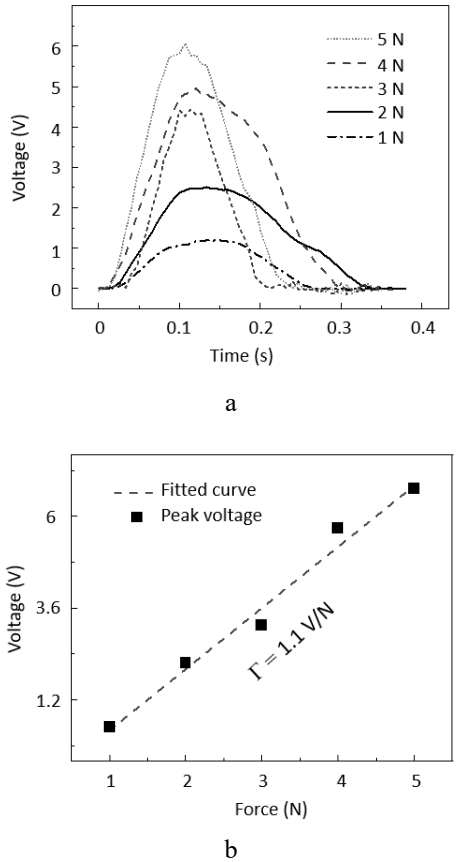

Fig. 3 Measurements of the hit force stimulated voltage signal on the on-racket flexible sensors: a – signal caused by different force pulses, b – peak voltage with increased hitting force

size laser-cut cave; the interface circuit were assembled parallel with the wood handle, which is also covered by a finely cut silicone rubber to filling the space and made as a flat cylinder; a thin layer of soft polyvinyl chloride film was then laid over the sensor surface and the racket handle, which would protect the PVDF sensor and make the handling more comfortable. The total weight of the racket and monitoring system is ~250 g, while the raw racket has a weight of 167 g. The width of handle reached 32mm, which was wider than its original width of 25 mm. However, these parameters are still in the range for the normal table tennis racket and can be optimized in future production. Although integrated into a single board, there exists potential for further integration of the lines, circuitry, and battery into an ultrathin form factor, particularly with the use of a specially designed racket [25]. Additionally, the battery module could potentially be replaced by a piezoelectric device to harness energy from the racket's movement.

To measure the kinetic energy of the table tennis ball, it's imperative to establish the relationship between hitting force and the generated electric voltage. The results of this force-electric potential relationship are depicted in Fig. 3, a. In this test, a force meter (HP-100) is employed to administer a designed force to the sensor. The force is applied in a pulse lasting 0.1 seconds, with a resolution of 0.01 N. Forces of varying intensities ranging from 1 N to 5 N are applied to one of the sensors, and the collected voltage over time is plotted. Despite potential influences from the sensor's surrounding environment, such as buffering effects altering the generated voltage, a discernible linear relationship between force and peak voltage is observed (as illustrated in Fig. 3, b. A linear function is fitted to the data, revealing a slope of 1.1 V/m. This relationship underscores the capability of sensor to measure different forces. Given that these forces stem from the kinetic power of the table tennis ball, it follows that the system can effectively measure the velocity of table tennis ball, which can in turn be utilized in fatigue status assessment.

3. Hitting Position Measurement and EMG Test

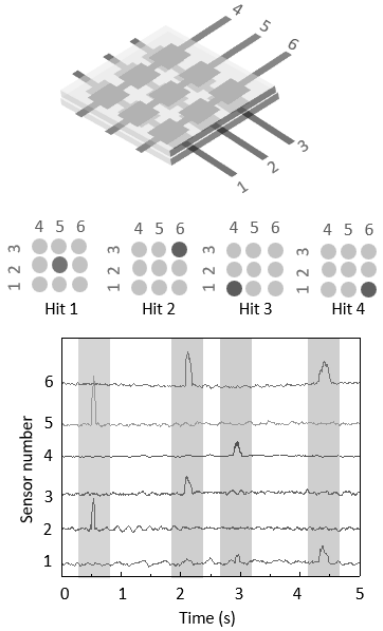

Fig. 4 Illustration of the sensor array structure (top row) and its ability for multipixel detection

The real table tennis hitting experiments was conducted using the fabricated measurement system to verify the system, and the resulting signals were recorded. The measured signals from four hits, along with the illustration of the hitting sensing, are shown in Fig. 4. During each hit, signals are generated from both the top and bottom sensor layers, allowing the hitting position to be determined at the intersection of the maximum voltage signals from both layers. Taking the first hit in Fig. 4 as an example, the maximum voltage from the bottom layer occurs at sensor 2, while the maximum voltage from the bottom layer occurs at sensor 5. The hitting position is then identified as the sensor at the intersection of column two and row two, as illustrated in Fig. 4. The other hitting positions can also be traced by the same analysis. Besides the positions, it can also be found that the sensors at the bottom layer will always generate a smaller signal than the top, of which the reason is the energy will be lost during the hitting force transmission. Both those information will be useful during the training of the kNN algorithm and the muscle status analysis [26, 27].

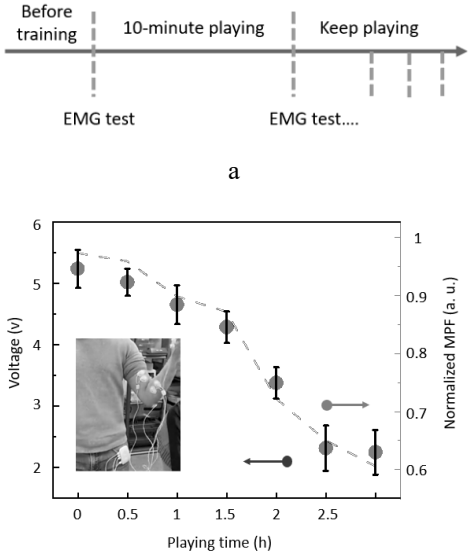

Fig. 5 EMG measurement for kNN training: a – the timeline for EMG measurement in data collection; b – change of the measured peak voltage and MPF data of EMG signal with playing times (error bars represent standard deviation)

Monitoring and drawing a conclusion for the muscle statute is not easy, while EMG-measured electrical activity of the muscle has been proven effective in demonstrating it [17]. As a result, we also conducted an EMG test to collect the data for the training. The decrease of mean power frequency (MPF) value in EMG test has been proved showing a higher fatigue of the muscle [18]. As we applied the designed pressure monitoring system in table tennis training, in the comparison stage, an EMG test for the arm muscle was also applied to investigate their status. At the first stage, we recruited two volunteers for the test. One male volunteer aged 27 was using the racket with a monitoring system, while another 28-year-old male used a normal racket. All the data are collected from the 27-year-old volunteer, while his competitor is always another volunteer. During the table tennis playing, we measured the EMG signal of the 27-year-old volunteer after each 10 minutes of

playing (the procedure is shown in Fig. 5, a). For the EMG test, the measurement frequency is set as 1kHz and eight distributed channels are fixed on the arm. A mean power frequency (MPF) number was shown on the instrument (TeleMyo™ 2400T G2, PPB FusionLab Corp.) and recorded during every measurement. After 2 hours playing, the collected MPF value drops apparently and the 0.7 normalized value is chosen at the threshold of muscle statue. As for the pressure sensing, the maximum voltages from six sensing channels from each hitting are utilized as the record voltage signal. As the example for the used data, Table I displays the 12 examples. Only the maximum value in each hitting is used at the algorithm input. For example, in the first hitting, only values at the 2nd and 4th sensors are used in training. This pickup process represents a post-processing step for the collect data to build the kNN classification algorithm.

A notable observation from the data is that higher ball velocities correspond to larger voltage outputs. The measured peak voltages and the MPF values are shown in Fig. 5, b. It is clearly shown that with a longer playing time, the MPF and voltage decrease at the same time. Combining the results shown in Fig. 3, b, a clear conclusion shows up, that the smaller voltage is caused by the smaller hitting pressure of the ball, demonstrating the change of player statue from natural to fatigue. It is also hard to establish a strict linear relation between MPF value and the generated voltage from the real experiment data. One reason is during the playing, not only the velocity but also the rotation of the ball is influenced by the player status, where the latter is difficult to quantified. Another reason is the player status is not linearly dropped, where the general trend does down but may not be reflected in every test.

Table 1

Response voltage peaks of each sensor at 12 hits and the measured MPF in EMG test

Hitting number	Number of sensors						Sensing positions (bottom row, top column)	Normalized MPF in EMG test after hitting data collection
	1	2	3	4	5	6		
1	0	4.2	0	5.3	0	0	(2, 4)	1
2	3.2	0	0	4.9	0	0	(1, 4)	1
3	2.9	0	0	0	5.6	0	(1, 5)	1
4	0	1.8	0	0	5.3	0	(2, 5)	0.9
5	0	1.6	0	0	4.6	0	(2, 5)	0.9
6	2.1	0	0	0	0	4.6	(1, 6)	0.9
7	0	0	1.5	0	0	3.5	(3, 6)	0.8
8	0	0.9	0	2.2	0	0	(2, 4)	0.8
9	0	1.6	0	0	0	2.5	(2, 6)	0.7
10	0	0	1.3	2.6	0	0	(3, 4)	0.6
11	0	0.3	0	0	1.3	0	(2, 5)	0.5
12	0	0	1.2	0	0	1.9	(3, 6)	0.6

Table 2

kNN algorithm table

Data: peak voltage of the top layer sensors (x_n), peak voltage of the bottom layer sensors (y_m), training label ($k_n = 0$ when MPF<0.7, $k_n = 1$ when MPF<0.7)

Result: threshold voltage x_0, y_0

Start $x_0 = x_1$; $y_0 = y_1$;

$$\delta = \sum_{i=1}^{n}\left(x_0 - x_i\left(k_n = 0\right)\right)^2 + \sum_{i=1}^{n}\left(x_0 - x_i\left(y_n = 1\right)\right)^2 ; \eta = \sum_{j=1}^{m}\left(y_0 - y_i\left(k_m = 0\right)\right)^2 + \sum_{j=1}^{m}\left(y_0 - y_i\left(k_m = 1\right)\right)^2$$

for $i = 2$ to $i=n$, $j = 2$ to $j=m$

$$\Delta = \sum_{l=1}^{n}\left(x_i - x_l\left(k_n = 0\right)\right)^2 + \sum_{j=1}^{n}\left(x_i - x_j\left(y_n = 0\right)\right)^2 + \sum_{g=1}^{m}\left(y_j - y_g\left(k_m = 0\right)\right)^2 + \sum_{g=1}^{m}\left(y_0 - y_g\left(k_m = 1\right)\right)^2$$

While $\Delta < \delta + \eta$,

do $x_0 = x_i$, $y_0 = y_i$;

end

4. kNN Method for Muscle Status Analysis

With the obtained voltage changes serving as inputs to the fatigue system, we proceed to implement the kNN algorithm. The training process of the kNN algorithm is outlined in Table II. This method categorizes input data into different groups based on their proximity to the training data. Although more sophisticated machine learning techniques have been developed, the kNN method suffices for our primary research and yields promising results [28, 29]. We collected 500 times hits from stage 1 test and labelled them as 0 when MPF < 0.7 and 1 when MPF > 1. The data set is then divided as two groups: 80% of them are used for training of the model and 20% of them are used in the test. During the training process, voltage threshold values for top and bottom layer are the output of the model, which are used to distinguish the fatigue status of them in the testing procedure. In the test of the classification, the accuracy and precision are calculated to evaluate the method. On the other hand, it should be noted that the embedded monitoring system will change the properties of the table tennis racket, hence changing the playing activity. But our analysis is based on the data measured by the designed racket. The method can also be migrated to other different or personalized data sets. Hence, the change of the racket because of the integration of the monitoring system will not influence the analysis results.

In Fig. 6, a, the classification results for 25 hits in testing group are displayed. Only top layer data x_n is plotted and the data points are labelled by their MPF value and arranged according to their respective sensing positions. Algorithm output threshold value x_0 is also marked as a dashed line. It is shown that kNN algorithm can effectively separate the obtained data for energetic (at the begin of the playing, normalized MPF>0.7) and fatigue (after 2 hours playing, normalized MPF<0.7) statues, underscoring the efficacy of using wearable devices with kNN method in discriminating fatigue levels. Furthermore, the distribution of hitting positions, where the maximum voltage is obtained from the system, varies across the racket surface. Central middle sensors, such as (2, 4), (2, 5) and (2, 6), register more hits compared to others, indicating that players predominantly utilize the center area of the racket during gameplay. These data can also be used in the future algorithm to do the further analysis of table tennis playing. To verify the system more accurately, we repeated the stage 1 tests on 20 volunteers, including both table tennis game and the EMG test. During the test, all the variables are kept same with only change of playing time. After going through the same data processing, different threshold values for different volunteers are obtained, where these thresholds are used to discriminate the status of players. Compared with the MPF measurement results measuring during the playing, the 500×20 date points can be used to calculate the accuracy and precision of the system using the equation [28]:

$$Accuracy = \frac{TP + TN}{TP + TN + FP + FN} \times 100\%, \quad (1)$$

$$Precision\_N = \frac{TN}{TN + FN} \times 100\%, \quad (2)$$

$$Precision\_P = \frac{TP}{TP + FP} \times 100\%, \quad (3)$$

where *TP*, *TN*, *FN*, *FP* are true positive, true negative, false negative, and false positive values, respectively, which is the number for true classification for MPF < 0.7, true classification for MPF > 0.7, false classification for MPF>0.7, false classification MPF<0.7 in this work. By applying this equation, it is determined that the system achieves an accuracy of 95%. *Precision_N* is for the right classification for the data measured at the beginning of the measurement and *Precision_P* is for the classification for after two hours of playing. The calculated precision value is shown in Fig. 6, b, which shows the prediction precision are both higher than 90%. Besides the prediction for playing time, the method also holds further potential for applications such as player identification by using the threshold boundary information or training guidance using the real-time monitoring feature of the system [30, 31].

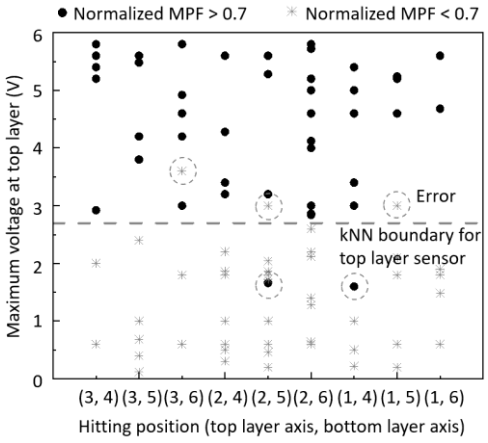

a

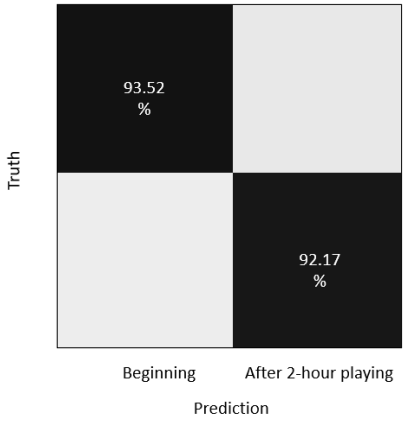

b

Fig. 6 kNN classification and results: a – measured voltages from top layer sensors and kNN algorithm result, the errors are also marked in the figure, b – calculated precision chart for the true prediction using all the data

5. Conclusions

In conclusion, the table tennis monitoring system is integrated directly into the racket, utilizing a kNN algorithm for data process to know the player's status. This monitoring system incorporates a flexible piezoelectric sensing array to capture hitting position and pressure. One position on the racket is decomposed into row and column axes, with only one single striped PVDF (Polyvinylidene fluoride) flexible electrode placed on each axis. By using this strategy, only 3+3 signal channels are needed for sensing 3×3 sensing array. The pressure exerted is directly proportional to the energy transferred from the racket to the ball, thereby reflecting the player's muscle status, which is also verified by the EMG test. Following training of a kNN algorithm using EMG data marked sensing voltage data, the system can detect fatigue levels with high accuracy. This design verifies the row-column sensing method to reduce communication channels and the combination of hardware innovation and algorithm design, which will benefit various applications, including health monitoring, sports training, and AI-based data acquisition.

References

1. **Nahavandi, D.; Alizadehsani, R.; Khosravi, A.; Acharya, U. R.** 2022. Application of artificial intelligence in wearable devices: Opportunities and challenges, Computer Methods and Programs in Biomedicine 213: 10654. https://doi.org/10.1016/j.cmpb.2021.106541.

2. **Jin, C. Y.** 2019. A review of AI Technologies for Wearable Devices, IOP Conference Series: Materials Science and Engineering 688: 044072. https://doi.org/10.1088/1757-899X/688/4/044072.
3. **Hu, H.; Huang, H.; Li, M.; Gao, X.; Yin, L.; Qi, R.; Wu, R. S.; Chen, X.; Ma, Y.; Shi, K.; Li, C.; Maus, T. M.; Huang, B.; Lu, C.; Lin, M.; Zhou, S.; Lou, Z.; Gu, Y.; Chen, Y.; Lei, Y.; Wang, X.; Wang, R.; Yue, W.; Yang, X.; Bian, Y.; Mu, J.; Park, G.; Xiang, S.; Cai, S.; Corey, P. W.; Wang, J.; Xu, S.** 2023. A wearable cardiac ultrasound imager, Nature 613: 667-675. https://doi.org/10.1038/s41586-022-05498-z.
4. **Ahmed, A.; Aziz, S.; Abd-alrazaq, A.; Farooq, F.; Sheikh, J.** 2022. Overview of Artificial Intelligence–Driven Wearable Devices for Diabetes: Scoping Review, Journal of Medical Internet Research 24(8): e36010. https://doi.org/10.2196/36010.
5. **Abd-alrazaq. A.; AlSaad, R.; Harfouche, M.; Aziz, S.; Ahmed, A.; Damseh, R.; Sheikh, J.** 2023. Wearable Artificial Intelligence for Detecting Anxiety: Systematic Review and Meta-Analysis, Journal of Medical Internet Research 25: e48754. https://doi.org/10.2196/48754.
6. **Wu, J.; Fan, Z.** 2024. Portable Referee System for Volleyball Game Based on Pressure Monitoring and Self-Powering Communication, Mechanika 30(1): 91-96. https://doi.org/10.5755/j02.mech.33756.
7. **Yu, K.; Gong, Y.; Fan, Z.** 2022. A Battery-free Pressure Sensing System Based on Soft Piezoelectric Device for Tennis Training, Mechanika 28(3): 237-241. https://doi.org/10.5755/j02.mech.30459.
8. **Zhang, D.; Liu, J.; Yao, J.; Zhang, Z.; Chen, B.; Lin, Z.; Cao, J.; Wang, X.** 2022. Enhanced Sub-Terahertz Microscopy based on Broadband Airy Beam, Advanced Materials Technologies 7(5): 2100985. https://doi.org/10.1002/admt.202100985.
9. **Zhang, D.; Wang, B.; Wang, X.** 2019. Enhanced and modulated microwave-induced thermoacoustic imaging by ferromagnetic resonance, Applied Physics Express 12(7): 077001. https://doi.org/10.7567/1882-0786/ab265d.
10. **Ostaševičius, V.; Jūrėnas, V.; Karpavičius, P.; Baskutienė, J.** 2017. Self-powered wireless sensor system application for cutting process control, Mechanika 23(3): 456-461. https://doi.org/10.5755/j01.mech.23.3.17957.
11. **Li, J.; Wang, B.; Zhang, D.; Li, C.; Zhu, Y.; Zou, Y.; Chen, B.; Wu, T.; Wang, X.** 2021. A Preclinical System Prototype for Focused Microwave Breast Hyperthermia Guided by Compressive Thermoacoustic Tomography, IEEE Transactions on Biomedical Engineering, 68(7): 2289-2300. https://doi.org/10.1109/TBME.2021.3059869.
12. **Lin, Z.; Pan, X.; Yao, J.; Wu, Y.; Wang, Z.; Zhang, D.; Ye, C.; Xu, S.; Yang, F.; Wang, X.** 2021. Characterization of Orbital Angular Momentum Applying Single-Sensor Compressive Imaging Based on a Microwave Spatial Wave Modulator, IEEE Transactions on Antennas and Propagations 69(10): 6870-6880. https://doi.org/10.1109/TAP.2021.3070067.
13. **Bestwick-Stevenson, T.; Toone, R.; Neupert, E.; Edwards, K.; Kluzek, S.** 2022. Assessment of Fatigue and Recovery in Sport: Narrative Review, International Journal of Sports Medicine 43(14): 1151-1162. https://doi.org/10.1055/a-1834-7177.
14. **Pareja-Blanco, F.; Alcazar, J.; Sánchez-Valdepeñas, J.; Cornejo-Daza, P. J.; Piqueras-Sanchiz, F.; Mora-Vela, R.; Sánchez-Moreno, M.; Bachero-Mena, B.; Ortega-Becerra, M.; Alegre, L. M.** 2020. Velocity Loss as a Critical Variable Determining the Adaptations to Strength Training, Medicine and Science in Sports and Exercise 52(8): 1752-1762. https://doi.org/10.1249/mss.0000000000002295.
15. **Thorpe, R. T.; Atkinson, G.; Drust. B.; Gregson, W.** 2017. Monitoring Fatigue Status in Elite Team-Sport Athletes: Implications for Practice, International Journal of Sports Physiology and Performance 12(s2): 27-34. https://doi.org/10.1123/ijspp.2016-0434.
16. **Weakley, J.; Mann, B.; Banyard, H.; McLaren, S.; Scott, T.; Garcia-Ramos, A.** 2021. Velocity-Based Training: From Theory to Application, Strength and Conditioning Journal 43(2): 31-49. https://doi.org/10.1519/SSC.0000000000000560.
17. **Cifrek, M.; Medved, V.; Tonković, S.; Ostojić, S.** 2009. Surface EMG based muscle fatigue evaluation in biomechanics, Clinical Biomechanics 24(4): 327-340. https://doi.org/10.1016/j.clinbiomech.2009.01.010.
18. **Balsalobre-Fernández, C.; Marchante, D.; Baz-Valle, E.; Alonso-Molero, I.; Jiménez, S. L.; Muñóz-López, M.** 2017. Analysis of Wearable and Smartphone-Based Technologies for the Measurement of Barbell Velocity in Different Resistance Training Exercises, Frontiers in Physiology 8: 649. https://doi.org/10.3389/fphys.2017.00649.
19. **Iino, Y.; Kojima, T.** 2009. Kinematics of table tennis topspin forehands: effects of performance level and ball spin, Journal of Sports Sciences 27(12): 1311-1321. https://doi.org/10.1080/02640410903264458.
20. **Dagdeviren, C.; Joe, P.; Tuzmanc, O. L.; Park, K.; Lee, K. J.; Shi, Y.; Huang, Y.; Rogers, J. A.** 2016. Recent progress in flexible and stretchable piezoelectric devices for mechanical energy harvesting, sensing and actuation, Extreme Mechanics Letters 9: 269-281. https://doi.org/10.1016/j.eml.2016.05.015.
21. **Zhang D. J.; Su, J.; Lu, C. J.; Zhang, Y. C.; Zhang, C.; Li, Y.; Feng, L. Y.** 2017. Room-temperature multiferroic properties of sol-gel derived $0.5LaFeO_3$-$Bi_4Ti_3O_{12}$ thin films with layered perovskite, Journal of Alloys and Compounds 709:729-734. https://doi.org/10.1016/j.jallcom.2017.03.140.
22. **Tian, G.; Deng, W.; Gao, Y.; Xiong, D.; Yan, C.; He, X.; Yang, T.; Jin, L.; Chu, X.; Zhang, H.; Yan, W.; Yang, W.** 2019. Rich lamellar crystal baklava-structured PZT/PVDF piezoelectric sensor toward individual table tennis training, Nano Energy 59: 574-581. https://doi.org/10.1016/j.nanoen.2019.03.013.
23. **Zhang D.; Lin, Z.; Liu, J.; Zhang, J.; Zhang, Z.; Hao, Z. C.; Wang, X.** 2020. Broadband high-efficiency multiple vortex beams generated by an interleaved geometric-phase multifunctional metasurface, Optical Materials Express 10(7): 1531-1544. https://doi.org/10.1364/OME.395721.
24. **Li, Z.; Kong, X.; Zhang, J.; Shao, L.; Zhang, D.; Liu, J.; Wang, X.; Zhu, W.; Qiu, C. W.** 2022. Cryptography Metasurface for One-Time-Pad Encryption and Massive

Data Storage, Laser and Photonics Reviews, 16(8): 2200113.
https://doi.org/10.1002/lpor.202200113.
25. **Stassen, I.; Burtch, N.; Talin, A.; Falcaro, P.; Allendorf, M.; Ameloot, R.** 2017. An updated roadmap for the integration of metal–organic frameworks with electronic devices and chemical sensors, Chemical Society Reviews 46(11): 3185-3241.
https://doi.org/10.1039/c7cs00122c.
26. **Guo, G.; Wang, H.; Bell, D.; Bi, Y.; Greer, K.** 2003. KNN Model-Based Approach in Classification, In: Meersman, R.; Tari, Z.; Schmidt, D. C. (eds) On The Move to Meaningful Internet Systems 2003: CoopIS, DOA, and ODBASE. OTM 2003, Lecture Notes in Computer Science vol 2888: 986-996.
https://doi.org/10.1007/978-3-540-39964-3_62.
27. **Ashley, K.** 2020. Applied Machine Learning for Health and Fitness: A Practical Guide to Machine Learning with Deep Vision, Sensors and IoT. APress. 259p.
https://doi.org/10.1007/978-1-4842-5772-2.
28. **Fleuren, L. M.; Klausch, T. L. T.; Zwager, C. L.; Schoonmade, L. J.; Guo, T.; Roggeveen, L.; Swart, E. L.; Girbes, A. R. J.; Thoral, P.; Ercole, A.; Hoogendoorn, M.; Elbers, P. W. G.** 2020. Machine learning for the prediction of sepsis: a systematic review and meta-analysis of diagnostic test accuracy. Intensive care medicine, 46:383-400.
https://doi.org/10.1007/s00134-019-05872-y.
29. **Ripoll, H.; Kerlirzin, Y.; Stein, J.-F.; Reine, B.** 1995. Analysis of information processing, decision making, and visual strategies in complex problem solving sport situations, Human Movement Science 14(3): 325-349.
https://doi.org/10.1016/0167-9457(95)00019-O.
30. **Lin, Z.; Pan, X.; Yao, J.; Wu, Y.; Wang, Z.; Zhang, D.; Ye, C.; Xu, S.; Yang, F.; Wang, X.** 2021. Characterization of Orbital Angular Momentum Applying Single-Sensor Compressive Imaging Based on a Microwave Spatial Wave Modulator, IEEE Transactions on Antennas and Propagation 69(10): 6870-6880.
https://doi.org/10.1109/TAP.2021.3070067.
31. **Yamashita, T.; Kobayashi, T.** 2021. Smart Table Tennis Racket Using a Rubber Mounted Ultrathin Piezoelectric Sensor Array, Sensors and Materials 33(3): 1081-1089.
https://doi.org/10.18494/SAM.2021.2954.

C. Hua, X. Hu, Z. Fan, W. Fei

LESS SIGNAL CHANNEL TABLE TENNIS HITTING MEASUREMENT SYSTEM ENA-BLED MUSCLE CONDITION MONITORING

S u m m a r y

Sports play a crucial role in daily life, and precise monitoring of muscle states during sports is valuable for guiding training programs, preventing injuries, and detecting fouls. Despite significant advancements in monitoring technologies, there are still unexplored areas in detecting various sports actions and processing the associated data. In this study, we present a method to reduce communication channels in a table tennis racket sensor array and use the fabricated monitoring system to detect the player's status through signal analysis and machine learning algorithms. The system includes a flexible piezoelectric PVDF sensor array, Bluetooth chip, and battery. Unlike conventional designs that assign an individual communication channel to each sensor, this approach uses a single striped sensor on each row and column. By analyzing the axis of the sensor with signal, the hitting position and force are determined. After that, a kNN classification algorithm are built with the help of electromyography (EMG) test, aiming to assess the player's status based on their hitting input. The system effectively differentiates various player statuses with an accuracy exceeding 90%. The hardware innovation and signal processing techniques also have potential applications in other wearable sensing fields.

Keywords: piezoelectric sport monitoring system, less communication signal channel, table tennis game, muscle status analysis.

Received February 10, 2025
Accepted August 22, 2025